Molecular Crystals and Liquid Crystals

Publication details, including instructions for authors and subscription information:
http://www.tandfonline.com/loi/gmcl20

In Vitro Behavior of Ti-6Al-7Nb Alloy After Various Surface Treatments Modification

Vasilica Mihaela Mindroiu [a], E. Cicek [a] & Raluca Ciubar [b]

[a] Faculty of Applied Chemistry and Materials Science, University Politehnica of Bucharest, Polizu, Bucharest, Romania

[b] Research Center for Biochemistry and Molecular Biology, University of Bucharest, Independenței, Bucharest, Romania

Version of record first published: 22 Sep 2010

To cite this article: Vasilica Mihaela Mindroiu, E. Cicek & Raluca Ciubar (2008): In Vitro Behavior of Ti-6Al-7Nb Alloy After Various Surface Treatments Modification, Molecular Crystals and Liquid Crystals, 486:1, 120/[1162]-132/[1174]

To link to this article: http://dx.doi.org/10.1080/15421400801917874

Mol. Cryst. Liq. Cryst., Vol. 486, pp. 120/[1162]–132/[1174], 2008

ISSN: 1542-1406 print/1563-5287 online
DOI: 10.1080/15421400801917874

In Vitro Behavior of Ti-6Al-7Nb Alloy After Various Surface Treatments Modification

Vasilica Mihaela Mindroiu[1], E. Cicek[1], and Raluca Ciubar[2]
[1]Faculty of Applied Chemistry and Materials Science, University Politehnica of Bucharest, Polizu, Bucharest, Romania
[2]Research Center for Biochemistry and Molecular Biology, University of Bucharest, Independenţei, Bucharest, Romania

The paper is a new approach of in vitro behavior of Ti-6Al-7Nb bioalloy after various surface treatments and their correlation with corrosion and topographical properties and it could be useful for implant procedures. The morphology structure and wettability of the treated materials were investigated, as well as their corrosion behavior in simulated body fluid. Osteoblast culture and cell viability test were performed.

Keywords: cell culture; impedance spectroscopy; surface modification; Titanium alloys; wettability test

1. INTRODUCTION

Titanium and its alloys are widely used in dentistry and orthopedics ought to their outstanding biocompatibility and mechanical properties. Their interaction with cells depends most on surface properties (crystallographic structure, morphology and composition of surface layers, wettability) and on metal ion release. It has been established that the corrosion products may affect cell metabolism, that is, the corrosion current may affect cell behavior [1]. They spontaneously form in air an oxide layer containing dense and stable TiO_2, with a thickness of a few nanometers [2], which is responsible both for alloys corrosion resistance and their biocompatibility [3,4]. Moreover, this film favors also a very good osseointegration [5].

Address correspondence to Vasilica Mihaela, Mindroiu, University Politehnica of Bucharest, Faculty of Applied Chemistry and Materials Science, Polizu no 1-7, Bucharest 011061, Romania. E-mail: mihaela_istratescu@yahoo.com

Macroscopically modifications in morphology are often used to obtain a better connection: surface is made porous by plasma-pray coating or simply rougher by blasting, or covered with titanium beads [6,7]. Plasma spray is an expensive technique and it was reported that plasma-sprayed hydroxyapatite (HA) coating enhance implant performance at an early stage after implantation, but caused poorer long-term performances because of low adhesion of the coating to the metal and low crystallinity of the HA [6,7]. Some simple chemical, electrochemical and thermal treatments have been developed and tested in order to modify composition and morphology of surface layers, leading to a moderate bioactive behavior [8–12]. These surfaces are characterized by a sub-micrometric or nanometer texture.

In the present study, the properties of oxide films grown by chemical, electrochemical and thermal processes on Ti6Al7Nb have been investigated in simulated physiological solution by DC polarization and AC impedance spectroscopy techniques. Morphology structure and wettability of the treated and untreated surfaces were investigated and cytotoxicity test was performed, followed by a wide in vitro characterization based on osteoblast cell culture.

2. MATERIALS AND METHODS

2.1. Materials

A Ti6Al7Nb titanium alloy for prosthetic implants (composition given in Table 1) was employed; all experiments were carried out on disk-shaped samples (1 cm diameter, 2 cm thickness).

Their surface was polished to a finish (Ra = 1 μm), grinding paper to silica carbur with diverse granular meters. The electrodes were immersed in benzene for 5 minutes, after that were washed with distillated water and surface was treated in one of three ways:

– 30% nitric acid, then aged in boiling distilled water for 8 h [13];
– Anodic oxidation in H_2SO_4 solution 3M [14] by cronoamperometric method at 5 A;
– Heat treatment in air, 2 h at 600°C in a standard electric furnace [15].

TABLE 1 Composition of the Ti-6Al-7Nb Alloy

Element	Ti	Al	Nb	Fe	H	N	O	C
(wt% values)	rest	5.88	6.65	0.3	0.0121	0.05	0.2	0.1

Measurements of the corrosion behavior of treated and untreated Ti6Al7Nb alloys were performed in aerated simulated physiological Hank's Balanced Salt Solution (HBSS) [16] containing (in gL^{-1}): 8 NaCl, 0,4 KCl, 0.35 $NaHCO_3$, 0.25 $NaH_2PO_4 \cdot H_2O$, 0.06 $Na_2HPO_4 \cdot 2H_2O$, 0.19 $CaCl_2 \cdot 2H_2O$, 0.19 $MgCl_2$, 0.06 $MgSO_4 \cdot 7H_2O$, 1 glucose, at pH = 6.9.

2.2. Surface Characterization

Surface morphology and composition were assessed by Environmental Scanning Electron Microscope FEI/Phillps XL30 ESEM, pressure 0.7 Torr, and GSE conditions (water vapors). The equipment has an EDAX (energy-dispersive X-ray microanalysis) module.

2.3. Wettability Tests

Contact angle measurements were carried out in order to evaluate the wettability of the surface-modified alloy as resulting of every treatment. An equal volume of distilled water was placed on every sample by means of micropipette, forming a drop or spreading on the surface. Photos were taken through lenses KSV Instruments LTD optical stage microscope equipped with CAM100 to record the shape of the drops and measure the contact angle.

2.4. Cycle Voltametry

The cycle voltammetry was recorded for untreated and treated Ti6Al7Nb alloys in HBSS, in the potential range covering −0.8 V to 4 V used an 40 Voltalab with computer interface. A saturated Ag/AgCl AgCl electrode was used as the reference electrode and a platinum electrode as the counter electrode.

2.5. Open Circuit Potential

The potential measurements were performed with METRIX 20 electronic voltammeter. Monitoring of the open circuit potential, E_{oc} was made after different periods, during 1333 exposure hours.

2.6. Electrochemical Impedance Spectroscopy (EIS)

The EIS measurements were carried out using a 40 Voltalab, which was connected to a three-electrode electrochemical cell. All measurements were performed in Hank's solution at 0 V potential. The frequency ranged from 10 kHz to 10 mHz, and the amplitude used

was set at 5 mV [17]. Results were presented in terms of Bode plots. The spectra were interpreted using the Z View program.

2.7. *In Vitro* Biocompatibility Tests

To reveal the biocompatibility of Ti6Al7Nb alloys it was compared the behavior of G292 osteoblasts grown on Ti6Al7Nb discs or on plastic tissue culture dishes, a widely used material specifically treated by the manufacturer to enhance cell growth. The cells were grown in DMEM (Dulbecco's Modified Eagle Medium) supplemented with 10% FBS (Fetal Bovine Serum) and antibiotics 100 U/ml penicillin and 100 μg/ml streptomycin at 37°C in atmosphere with 5% CO_2. The analysis was performed over a period of 48 h. The MTT test was used to evaluate the cell viability. The cell morphology and the adherence to the Ti6Al7Nb surface were analyzed by fluorescence microscopy.

3. RESULTS

3.1. Surface Characterization

The SEM images for all Ti6Al7Nb samples show that the surface does not look different in morphology; the thickness of the oxide layer formed is very small of a few nanometers [2].

In the Figure 1 were illustrated the results of the surface morphology characterization and the composition of the untreated and treated Ti6Al7Nb samples.

From X-ray emission spectrums (Fig. 2) is noticed that the amount of oxide from the untreated samples is by 6.67%, the thermal treated samples contain more amount of oxide (approximate 14.47%), the anodized samples contain 9.92% and the chemical treated samples contain 9.06% mass amount of oxide.

3.2. Wettability

In the Table 2, the contact angle measurement results are presented for all samples.

Chemical and electrochemical treatments showed a great influence on the surface wettability. Distilled water put on untreated samples formed a regular drop, with a contact angle of about 84°. After passivation (anodization and chemical treatment in HNO_3), the contact angle decreases to less 50°, the surface is much more easily wetted, resulting in a very low contact angle. The behavior of thermal treated samples is

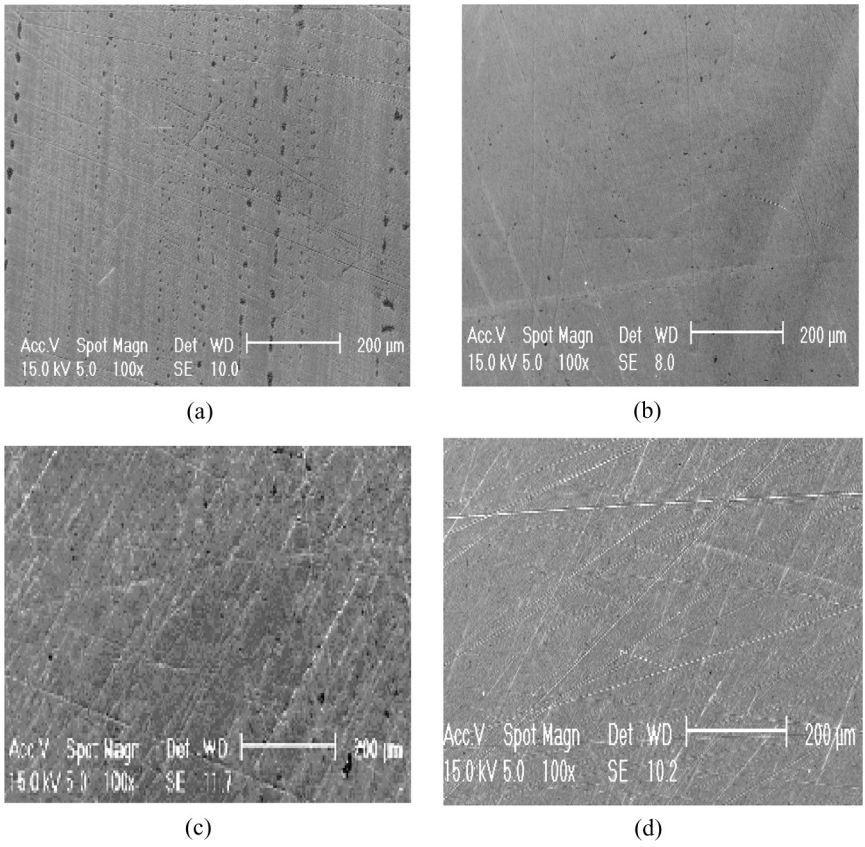

FIGURE 1 SEM images for: a) untreated; b) anodized; c) chemical and; d) thermal treated surface Ti6Al7Nb.

different than other treatments; the contact angle is bigger than untreated sample, Ti6Al7Nb alloys spontaneously form in air an oxide layer containing dense and stable TiO_2 [2].

3.3. Cycle Voltametry

The polarized curves of untreated and treated Ti6Al7Nb alloys obtained in HBSS are shown in Figure 3.

A typical anodic polarization curve generally consists of an active state, a passive state and a trans-passive state, but in our cases the active state is missing due to the preexisted oxide layer. In all cases, the material oxidation and the oxide layer formation were achieved.

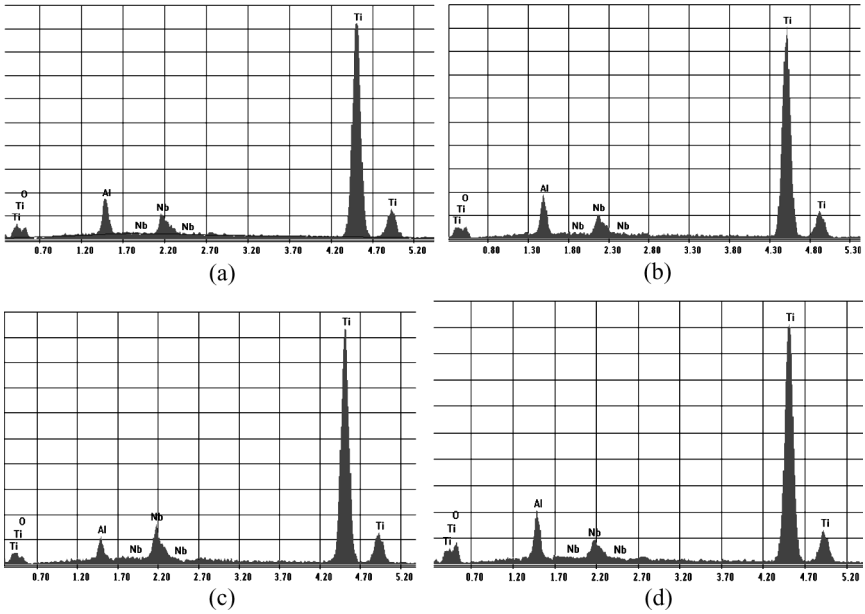

FIGURE 2 The X radiation emission spectrum for: a) untreated; b) anodized; c) chemical and; d) thermal treated surface Ti6Al7Nb.

The passive film is formed easily because the critical passivation current density is low and it is stable if the passivation holding current density is low.

In case of anodization treatment, the passive domain is larger than other treatments and for untreated alloy the passive state continued until 1.5 V.

The main electrochemical parameters of studied biomaterials like: corrosion potential (E_{cor}), corrosion current density (or corrosion rate) (i_{cor}) and polarization resistance (R_p) were determined by linear polarization method.

TABLE 2 The Results of Contact Angle Measurements

Material	CA (Contact angle) (°)
Untreated Ti6Al7Nb	84
Thermal treated Ti6Al7Nb	90
Anodized Ti6Al7Nb	23
Chemical treated Ti6Al7Nb	48

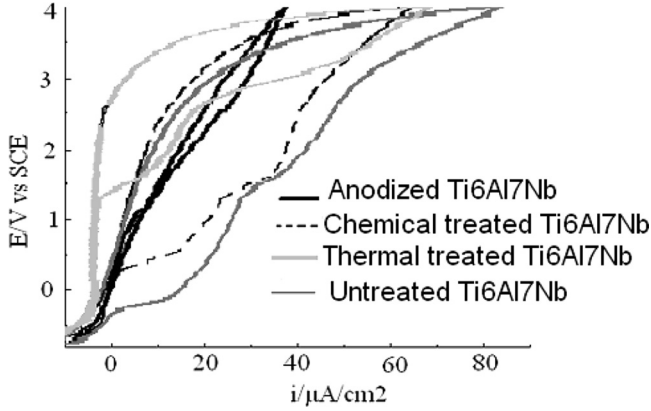

FIGURE 3 Cyclic voltammograms of untreated and treated Ti6Al7Nb alloys recorded in HBSS.

Results from Table 3 show that all passivation treatments improve the corrosion resistance of the alloy. The anodized Ti6Al7Nb alloy has highest polarization resistance, beside the corrosion rate is smaller than other treated samples ones.

3.4. Open Circuit Potential

Figure 4 shows the variation of corrosion potential (E_{cor}) in time for 56 immersion days in HBSS. For untreated Ti6Al7Nb alloy the initial corrosion potential value is around -216 mV, after 21 immersion days in HBSS the corrosion potential increases to less electronegative values around -82 mV, but after 22 immersion days the value decreases to -176 mV.

TABLE 3 Corrosion Parameters of Untreated and Treated Ti6Al7Nb Alloys Obtained from Polarization Curves in HBSS Achieved

Electrochemical parameters	Untreated Ti6Al7Nb	Anodized Ti6Al7Nb	Chemical treated Ti6Al7Nb	Thermal treated Ti6Al7Nb
E_{cor} (mV)	-315.8	149.5	-62.2	-170.3
R_p (Ω/cm^2)	$3.25 \cdot 10^5$	$6 \cdot 10^5$	$4.33 \cdot 10^5$	$4.16 \cdot 10^5$
I_{cor} ($\mu A/cm^2$)	$8.12 \cdot 10^{-2}$	$4.37 \cdot 10^{-2}$	$6 \cdot 10^{-2}$	$6.25 \cdot 10^{-2}$
V_{cor} (mm/Y)	$7.25 \cdot 10^{-4}$	$4 \cdot 10^{-4}$	$5.4 \cdot 10^{-4}$	$5.66 \cdot 10^{-4}$
Passive domain (mV)	1553	3500	1886	2462

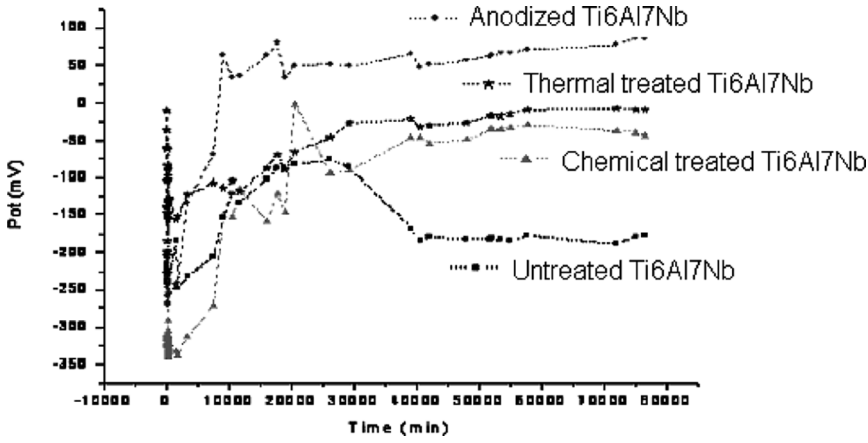

FIGURE 4 Corrosion potential evolution in time for untreated and treated Ti6Al7Nb alloys recorded in HBSS.

In case of anodized Ti6Al7Nb the initial corrosion potential value is around -199 mV (Ag/AgCl), and then it increases to more electropositive values, reaching to positive values around of 64 mV after 6 immersion days in HBSS.

The same tendency occurred in case of chemical treated Ti6Al7Nb in HNO_3, the initial corrosion value is more electronegative, around -311 mV, after 27 days in bio liquid immersion the corrosion potential seams to be stabilized around of -40 mV.

The initial corrosion potential value for thermal treated Ti6Al7Nb is around -103 mV and after 36 immersion days in HBSS the value of corrosion potential is stabilized around of -90 mV.

From Figure 4 it is note that the anodized Ti6Al7Nb alloy has the best corrosion behavior in HBSS, followed by thermal treated alloy and then by the chemical treated in HNO_3 Ti6Al7Nb alloy.

3.5. Electrochemical Impedance Spectroscopy (EIS)

The potential for investigation of the electrochemical behavior of the Ti-6Al7-Nb alloys by EIS measurements was chosen from the above polarization curves. It was decided to perform these tests at 0 mV (SCE).

The Bode plots of EIS measurements are shown in Figures 5 and 6. At last two relaxation time constants are indicated by the two peaks on all phase angle plots (Fig. 5). In Log Z Bode plots (Fig. 6) straight lines are observed with slope approaching -1, in a similar way as for other titanium alloys reported in literature [4,18].

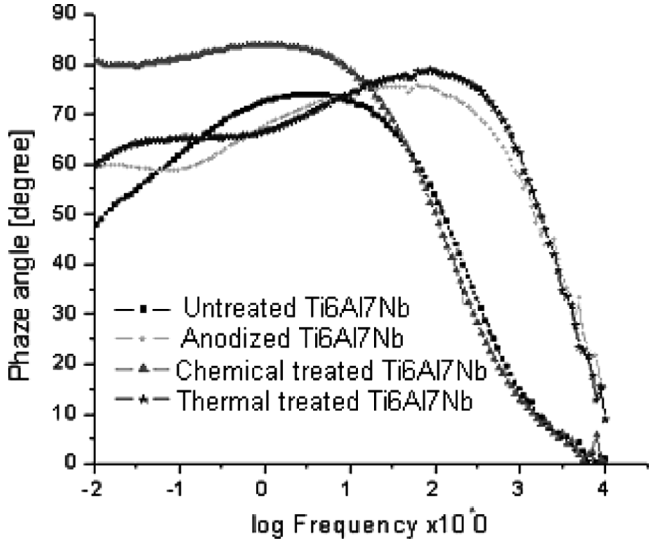

FIGURE 5 Phase angle Bode spectra for all Ti6Al7Nb alloys tested at potential 0 mV in Hank's solution at pH 7.8 and 25°C.

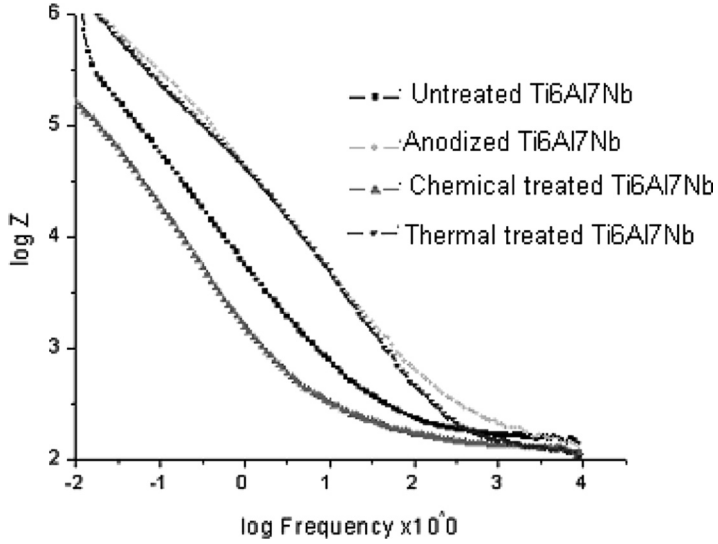

FIGURE 6 Z Bode spectra for all Ti6Al7Nb alloys tested at potential 0 mV in Hank's solution at pH 7.8 and 25°C.

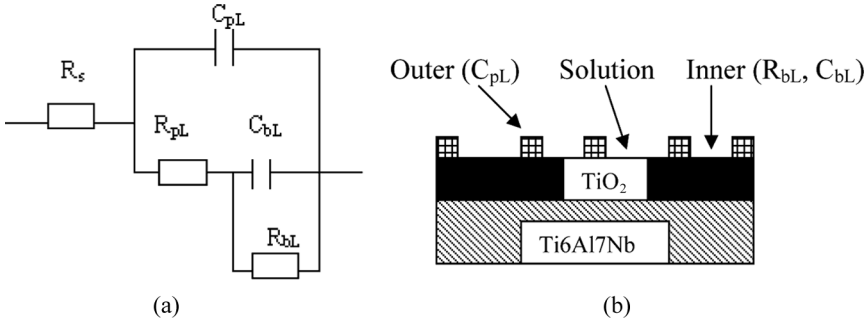

FIGURE7 a) Electrical equivalent circuit; b) schematic model of the bi-layer oxide film for Ti6Al7Nb alloy in Hank's solution.

The obtained spectra were interpreted in terms of an "equivalent circuit" (Fig. 7) whose the circuit elements, R_{bL} and $C_{bL,}$ represent the resistance and capacitance of the barrier layer, and R_{pL} and $C_{pL,}$ represent the resistance of the porous layer with the electrolyte inside the pores and the capacitance of the porous layer, respectively. R_s is the resistance of the Hank's solution. The results of the fitting are presented in Table 4.

For titanium oxide film, a distributed relaxation feature is commonly observed [3]. Due to this fact, in this study a constant phase element (CPE) was used for data adjustment instead of an ideal capacitor. The impedance of the CPE is given by $Z_{CPE} = C\ [(jw)]^{n-1}$, where C is the capacitance associated to an ideal capacitor, w is the angular frequency and $-1 < n < 1$ [19].

The high resistance of the barrier layer R_{bL} for all treatments implies a high corrosion resistance of the Ti-6Al-7Nb alloy in Hank's solution, i.e., a low rate of titanium release.

It is note that C_{bL} and C_{pL} have similar values for all treatments tested in this investigation. It is believed that the outer layer (porous)

TABLE 4 Electrical Parameters of Equivalent Circuit Obtained by Fitting the Experimental Results of EIS Test

Materials	R_s ($\Omega \cdot cm^2$)	C_{pL} ($\mu F \cdot cm^{-2}$)	R_{pL} ($k\Omega \cdot cm^2$)	C_{bL} ($\mu F \cdot cm^{-2}$)	R_{bL} ($k\Omega \cdot cm^2$)
Untreated Ti6Al7Nb	153	9.93	27.704	8.23	37.484
Anodized Ti6Al7Nb	119	1.6	234.9	1.46	296.8
Chemical treated Ti6Al7Nb	113	4.55	44.5	3.05	861.120
Thermal treated Ti6Al7Nb	116	1.37	56	1.03	160.58

consists of the same oxide as the inner layer (barrier) but with microscopic pores. The pores in the outer layer may be filled with electrolyte, and this might have contributed to the larger values of C_{pL} comparatively to C_{bL}.

3.6. *In Vitro* Biocompatibility Tests

Figure 8, the fluorescence images of osteoblasts cultured after 48 hours from seeding are illustrated.

Osteoblasts adhered on the alloy discs as well as on plastic. The morphology of cells on the samples analyzed was similar to that observed for the cells on plastic. After 48 hours of culture, the density of cells on the discs was elevated for anodized, chemically or thermal treated samples compared to untreated one. The MTT test showed

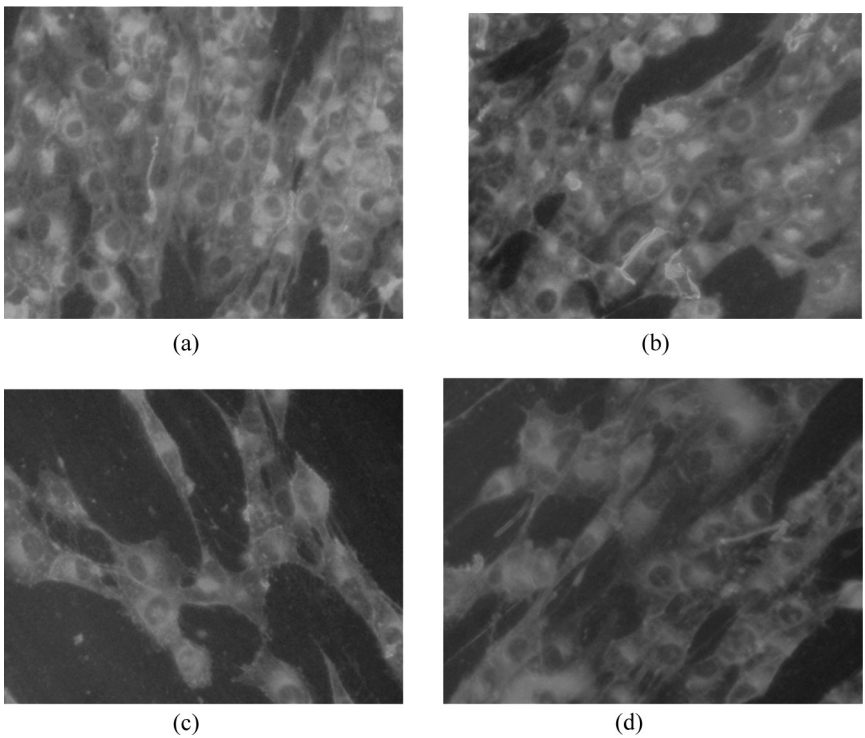

FIGURE 8 The fluorescence images of osteoblasts cultures on: a) anodized treated Ti6Al7Nb; b) chemical treated in HNO_3Ti6Al7Nb; c) untreated Ti6Al7Nb; d) thermal treated Ti6Al7Nb.

100% of cell viability in Ti6Al7Nb alloys, which eliminated the slightest adverse effect of ions release concern.

It is note that the cell density of Ti6Al7Nb anodized is more increase than untreated Ti6Al7Nb one.

CONCLUSION

1. The treatments promote the formation of a relative thick oxide layer with different structure and composition.
2. The all surface treatments increase the corrosion resistance of the Ti6Al7Nb alloy. The best efficiency is for anodized surface.
3. Related to impedance measurements in Hank's solution the two-layer oxide film is composed of a dense inner layer and a porous outer layer.
4. The MTT test shows approximately the same cell viability (100%) for all treated surfaces of Ti6Al7Nb alloy, despite the contact angle values which denote a various balance hydrophilic-hydrophobic.

REFERENCES

[1] Rogers, D., Howie, D. W., Graves, S. E., Pearcy, M. J., & Haynes, D. R. (1997). *J. Bone Joint Surg., B*, *79*, 311–315.
[2] Puleo, D. A. & Nanci, A. (1999). *Biomaterials*, *20*, 2311–2321.
[3] Pan, J., Thierry, D., & Leygraf, C. (1996). *Electrochem. Acta*, *41*, 1143.
[4] Gonzales, J. E. G. & Mirza-Rosca, J. C. (1999). *J. Electroanal. Chem.*, *471*, 109.
[5] Lavos-Valereto, I. C., Jr., König, B., Jr., Rossa, C., Jr., Marcantonio, E., Jr., & Zavaglia, A. C. (2001). *J. Mater. Sci. Mater. Med.*, *12*(3), 273–276.
[6] Lavos-Valereto, I. C., Deboni, M. C., & Azambuja, N. (2002). *J. Periodontol*, *73*(8), 900–905.
[7] Martini, D., Fini, M., Franchi, M., DePasquale, V., Bacchelli, B., Gamberini, M., Tinti, A., Giavaresi, G., Ottani, V., Raspanti, M., Giuzzardi, S., & Ruggeri, A. (2003). *Biomaterials*, *24*, 1309–1316.
[8] Kokubo, T., Miyaji, F., Kim, H. M., & Nakamura, T. J. (1996). *J. Am. Ceram. Soc.*, *79*, 1127–1129.
[9] Kokubo, T., Kim, H. M., & Kawashita, M. (2003). *Biomaterials*, *24*, 2161–2175.
[10] Jonasova, L., Müller, F., Helebrant, A., Strnad, J., & Greil, P. (2002). *Biomaterials*, *23*, 3095–3101.
[11] Strnad, J., Helebrant, A., & Mraz, R. (1999). *Materials for Medical Engineering EUROMAT '99*, 2, pp. 133–139.
[12] Wen, H. B., Liu, Q., De Wijn, J. R., De Groot, K., & Cui, F. Z. (1998). *J. Mater Sci: Mater Med.*, *9*, 121–128.
[13] Browne, M. & Greson, P. J. (2000). *Biomaterials*, *21*, 385–392.
[14] Chrzanowski, W. (2006). *Journal of Achievements in Materials and Manufacturing Engineering*, *18*, 67–70.
[15] Spriano, S., Bosetti, M., Bronzoni, M., Verne, E., Maina, G., Bergo, V., & Cannas, M. (2004). *Biomaterials*, *26*, 1219–1229.
[16] Metikos–Hukovic, M., Kwokal, A., & Piljac, J. (2003). *Biomaterials*, *24*, 3765–3775.

[17] Lavos-Valereto, I. C., Wolynec, S., Ramires, I., Guastaldi, A. C., & Costa, I. (2004). *Jurnal of Materials Science: Materials in Medicine*, *15*, 55–59.
[18] Silva, T. M., Rito, J. E., Simoes, A. M. P., Ferreira, M. G. S., Da Cunha Belo, M., & Watkins, K. G. (1998). *Electrochim. Acta*, *43*, 203–211.
[19] Gluszek, J., Masalski, J., Furman, P., & Nitsch, K. (1997). *Biomaterials*, *18*, 789–794.